Catal Lett (2008) 124:277–283
DOI 10.1007/s10562-008-9449-x

On the Role of Calcination Temperature in Pt-SO_4^{2-}/$ZrO_2-Al_2O_3$ Preparation and Catalytic Behaviors During the *n*-Hexane Hydroisomerization

X. L. Zhou · G. X. Yu · C. Tang · C. L. Li · J. A. Wang · O. Novaro · M. E. Llanos · Ma. A. Cortés-Jácome

Received: 18 January 2008 / Accepted: 19 February 2008 / Published online: 11 March 2008

Abstract Effects of calcination temperature for Pt-SO_4^{2-}/$ZrO_2-Al_2O_3$ (PSZA) catalysts in *n*-hexane hydroisomerization were investigated by N_2-adsorption, XRD, TG-DTA, FTIR, XPS and H_2-TPR. An optimum calcination temperature is helpful to complete the crystallization process, resulting in better distribution of alumina into zirconia crystal and producing new acid centers responsible for higher catalytic activity.

Keywords Calcination temperature · Hydroisomerization · Hexane · Zirconia sulfate · Lewis acid sites · Alumina

1 Introduction

n-Pentane and *n*-hexane (*n*-C_5/*n*-C_6) hydroisomerization is one of the most economical and efficient processes to produce high octane number gasoline composition. These reactions are limited by thermodynamic equilibrium, favoring at low temperatures. Platinum loaded mordenite and platinum loaded chlorinated alumina are two kinds of catalysts widely used in the industrial process. The latter catalyst can be operated at lower temperature producing gasoline components with higher octane number, but it needs frequently make-up organic chlorine components, resulting in corrosion and pollution problems. In addition, this catalyst is very sensitive to sulfur and water in the feedstock.

Sulfated zirconia (SZ) promoted with metal and/or cations demonstrated high catalytic activities in alkane hydroisomerization at low temperatures without the problems and feed limitations mentioned above [1–3]. However, it was often in powdered form with very poor mechanical properties; therefore, alumina must be added as a binder in industrial catalyst preparation. It was then discovered that introduction of alumina could markedly improve the catalyst performance [4–6]. Moreover, it is reported that promotion of platinum to SZ in PSZ preparation would not only inhibit the formation of coke improving the stability but also results in high steady yields of isomers in *n*-C_5/*n*-C_6 hydroisomerization [7, 8]. Therefore, promotion of alumina and platinum to SZ components has been considered to be a milestone to pave the way for industrial use of SZ catalysts [9, 10].

It was commonly recognized that proper calcination of Pt- and Al_2O_3-promoted SZ was a necessary step and it played the most important role to create the active sites in PSZ or PSZA catalysts for alkane isomerization [11–13]. Previous work has been tensely focused on the investigation of SZ or PSZ catalysts. Sohn et al. [14] and Comelli et al. [15] separately examined the effect of calcination temperature on SZ catalytic performance in C_4 isomerization and the concomitant changes in SZ crystalline structure. Chuah et al. [16]

X. L. Zhou · G. X. Yu (✉) · C. Tang · C. L. Li
Petroleum Processing Research Center, East China University of Science and Technology, 200237 Shanghai, P.R. China
e-mail: guoxianyu828@yahoo.com.cn

J. A. Wang
Laboratorio de Catálisis y Materiales, ESIQIE, Instituto Politécnico Nacional, Col. Zacatenco, 07738 Mexico D.F., Mexico

O. Novaro
Instituto de Física, Universidad Nacional Autónoma de México, A. P.20-364, 01000 Ciudad Universitario, México D.F., Mexico

M. E. Llanos · Ma. A. Cortés-Jácome
Instituto Mexicano del Petróleo, Programa de Ingeniería Molecular, Eje Central Lázaro Cárdenas No. 152, 07730 Mexico D.F., Mexico

paid more attention to changes in surface area at various calcination temperatures. Funamoto et al. [17] correlated SZ catalyst activity with Lewis acid sites and the intensity of $\nu_{S=O}$ at various calcination temperatures for n-C_4 isomerization under supercritical conditions by FTIR measurement. Hosoi et al. [18] and Comelli et al. [19] separately examined the effect of calcination conditions on n-C_5 and n-C_6 hydroisomerization behaviors over platinum-containing SZ catalysts (PSZ), but platinum was loaded before calcination in their preparation procedures that were different from an alternative method commonly used in the latest literatures [2, 20]. The latter was also accepted in this work. In Hosoi et al. and Comelli et al. works, no parallel correlation between acidity behaviors and activity in $n$$C_5$ or n-C_6 hydroisomerization on PSZ at varying calcination conditions was given. In addition, PSZA catalysts have potential industrial use in n-C_6 hydroisomerization. Preparation parameters for Al_2O_3-promoted SZ series catalysts (SZA) have already been investigated at a fixed calcination temperature in the literature [21], but the influence of calcination temperature on ZrO_2 crystallization process, active sites, action between Al and Zr, catalytic performance and their relationship for PSZA catalysts have not yet been reported in the published literature. In this paper, therefore, correlativity of physico-chemical properties and catalytic activities of PSZA catalysts at varying calcination temperatures has been dealt with. Optimum calcining temperature for SZA precursors in PSZA preparation was studied.

2 Experimental

2.1 Catalyst Preparation

A solution with zirconium content of 0.4 mol/L was prepared by dissolving $ZrOCl_2{\cdot}8H_2O$ in deionized water. A 26 wt.% ammonia solution was dropwise added into that solution at a rate of 0.5 mL/min up to pH of 10. The solution and precipitate were filtered after being aged for 24 h at 110 °C. The precipitate was washed with distilled water until the disappearance of chloride ions ($AgNO_3$ test), dried at 110 °C for 12 h. The obtained $Zr(OH)_4$ sample was shaped with boehmite (alumina wt.%, 76.2%; pore volume, 0.342 mL/g; surface area, 273 m^2/g). The latter was dried at 110 °C and then pulverized to particles smaller than 290 μm. Sulfation procedure was carried out by impregnation method with 0.5 M of H_2SO_4 solution (15 mL/g) under continuous stirring at room temperature for 12 h. The sulfated boehmite-$Zr(OH)_4$ was filtered without washing then dried overnight at 110 °C, and then the dry sulfated solid (designated as SZA3 where the number 3 denoted alumina content, the loading S is 2.47 wt.%) was separated into four portions. They were calcined at 550, 600, 650 and 700 °C, respectively. Subsequently, the above products were impregnated with H_2PtCl_6 solution using the incipient wetness technique, and the time remaining at ambient temperature is 24 h. It was then dried overnight at 110 °C before the final calcination at a fixed temperature of 525 °C for 2 h. The platinum content was 0.5 wt.%. The obtained Pt-$SO_4^{2-}/ZrO_2-Al_2O_3$ catalysts were designated as PSZA3-calcination temperature and these catalyst samples were orderly designated as PSZA3-550, PSZA3-600, PSZA3-650 and PSZA3-700 by their calcination temperature.

2.2 Catalyst Characterization

The surface areas and pore diameters of the catalysts were measured by N_2 adsorption–desorption isotherms method at −196 °C with a Mircomeritics ASAP 2010 instrument. Prior to analysis, each sample was degassed at 200 °C for 6 h under 10^{-3} Torr. Specific surface areas were calculated by BET method and the pore size distribution patterns were obtained from the analysis of the desorption portion of the isotherms using the BJH method.

The powder X-ray diffraction (XRD) patterns were recorded on a Rigaku D/Max 2550 X using Cu Kα (l = 0.154 nm) radiation in an operating mode of 40 kV and 30 mA. Data were collected from 2 theta = 5–75° in steps of 0.02°/s.

TG/DTA analyses were performed on a SDT-Q600 instrument (TA, USA) in flowing air with temperature ramp set at 10 °C/min in the 25–1,000 °C temperature range.

Fourier-transform infrared (FTIR) spectra of adsorbed pyridine were recorded on a Bruker IES-88 spectrometer. The sample was pressed to a 15 mm plate and put in a wafer. It was degassed in vacuum of 10^{-4} Torr at 450 °C for 2 h and lowered the temperature to 200 °C. Pyridine was adsorbed for 10 min and took 30 min for equilibrium. Then it was scanned after being vacuumed for 40 min. Then raised the temperature to 300 °C and recorded after 10 min for equilibrium. Same procedures were performed for 400 and 450 °C. The number of Brönsted and Lewis acid sites was calculated according to the integral area of the bands at 1,540 and 1,450 cm^{-1}, respectively.

H_2-temperature programmed reduction (TPR) experiments were performed in Auto Chem II (Micromeritics, USA). The heating rate was 10 °C/min from 50 to 900 °C using argon stream containing 7 vol.% hydrogen. The hydrogen consumption was measured by a Shimadzu GC-8A gas chromatograph, equipped with a thermal conductivity detector (TCD).

X-ray photoelectron spectroscopy (XPS) spectra were recorded on a THERMO-VG scalab 250 spectrometer equipped with Al Kα X-ray source (1,486.6 eV) and a hemispherical analyzer in a static condition. The base pressure during the analysis was 10^{-9} Torr.

2.3 Catalytic Activity Measurements

The *n*-hexane hydroisomerization reaction was carried out in a flow-type fixed-bed reactor loaded with 1.0 g of catalyst. Prior to the reaction, the catalyst sample was pretreated with flowing dry air (40 mL/min) at 450 °C for 3 h to remove water adsorbed on the surface. The system was cooled to 250 °C and the catalyst was reduced in flowing hydrogen for 3 h at 250 °C. Hydrogen and *n*-hexane mixture was then introduced into the reactor and hydroisomerization evaluations were performed under a total pressure of 2.0 MPa at the desired temperature with *n*-hexane weight hourly space velocity (WHSV) of 2.0 h^{-1} and a hydrogen/*n*-hexane molar ratio of 3. Products were monitored and analyzed using an on-line GC-920 gas chromatograph with FID detector and 50-m OV-101capillary column, and the temperature-program of analysis was carried.

3 Results and Discussion

3.1 Catalytic Activities

The *n*-hexane hydroisomerization reactions were performed over PSZA3 catalysts at the temperature ranging from 190 to 260 °C. The conversion and iso-hexane yields were given in Fig. 1. It is seen from Fig. 1a that the conversion over PSZA3-650 is the highest. The iso-hexane yield over PSZA3-650 reaches the maximum at 220 °C, as shown in Fig. 1b. The catalytic activity was decreasing in the order as: PSZA3-650 > PSZA3-600 > PSZA3-700 > PSZA3-550. So a maximum activity was achieved for the catalyst calcined at 650 °C.

3.2 Textural Properties and Crystalline Structure

Table 1 showed that the surface area of PSZA3 catalysts gradually decreased in increasing calcination temperatures and the decrease was significant from 550 to 600 °C. It was also seen that PSZA3-600 and PSZA3-650 catalysts have large pore diameters of 6.6–6.8 nm. Changes in pore diameter followed the order of: PSZA3-650 > PSZA3-600 > PSZA3-700 > PSZA3-550. It showed that suitable calcination temperature could help to form large pore structure.

XRD patterns of the four samples calcined at various temperatures were recorded in Fig. 2. Only a well-defined tetragonal phase crystalline structure appeared for the catalysts calcined at 550–650 °C, whereas a small peak at 2-theta of 28.18° appeared at 700 °C, indicating that trace amount of monoclinic phase was formed at higher calcination temperature. It has been commonly recognized that

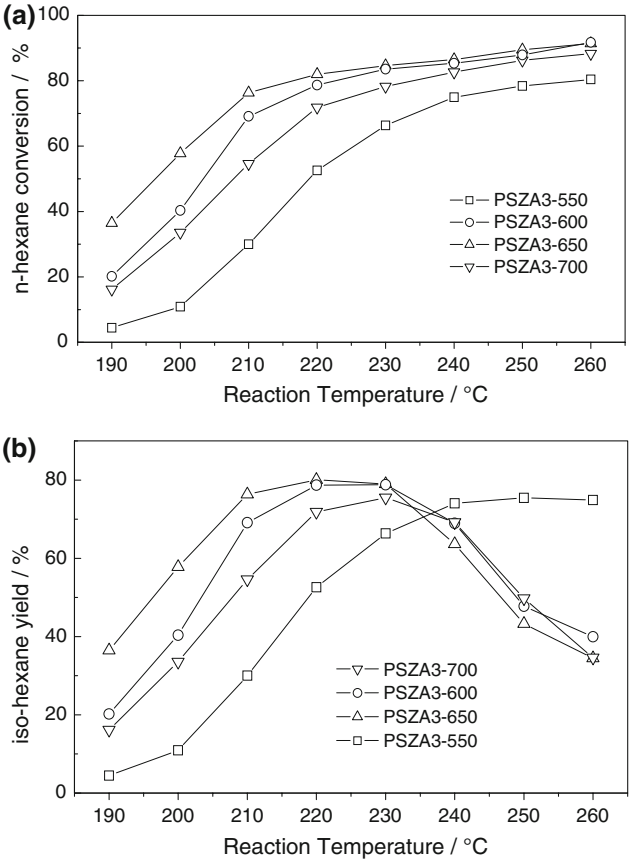

Fig. 1 Effect of reaction temperature on *n*-C_6 hydroisomerization over the PSZA3 catalysts (catalyst loading = 1.0 g; WHSV = 2.0 h^{-1}; reaction pressure P = 2.0 MPa; *n*-C_6:H_2 = 1:3)

Table 1 Textural properties of the catalysts

Catalysts	Calcination temperature (°C)	Surface area (m^2/g)	pore volume (mL/g)	pore diameter (nm)
PSZA3-550	550	162	0.135	3.43
PSZA3-600	600	113	0.150	6.60
PSZA3-650	650	109	0.138	6.82
PSZA3-700	700	95	0.141	5.93

only the tetragonal crystalline structure exhibited a higher catalytic activity for alkane isomerization [22, 23]. Therefore, tetragonal crystalline structure could be partially responsible for the high catalytic activities obtained on the catalysts PSZA3-600 and PSZA3-650.

Tetragonal zirconia plays one of the essential roles in highly active SZ catalyst series. Alumina in PSZA retarded the crystallization and stabilized the tetragonal zirconia phase [20, 24]. It is seen in Fig. 2 that the tetragonal phase structure was well formed around a calcination temperature of 600 and 650 °C, without monoclinic structure until 700 °C. These results demonstrated the optimum calcination temperature for PSZA3 should be about 650 °C.

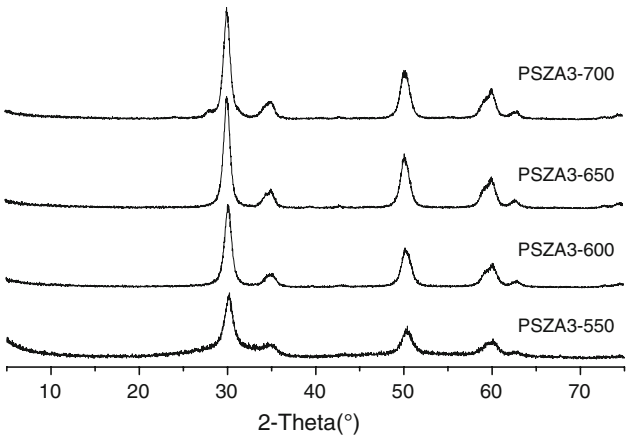

Fig. 2 XRD patterns of the samples

3.3 Thermal Analysis of $Zr(OH)_4$ and SZA3 Before Calcination

Thermal analysis results for $Zr(OH)_4$ and SZA3 before calcination were presented in Fig. 3 where Fig. 3a showed curves of $Zr(OH)_4$ and Fig. 3b showed that of SZA3 before calcination. From the former, it was observed that the TG curve of $Zr(OH)_4$ exhibited two main weight loss regions including: (i) The first stage, a strongly endothermic process at about 100 °C resulting from the removal of physic-adsorbed water. (ii) The second stage ranging 200 and about 430 °C assigned to an initial dehydroxylation step. It was also seen from TG curves in Fig. 3b that SZA3 before calcination exhibited three main weight loss regions including: (i) The first weight loss stage, a strongly endothermic process at about 100 °C resulting from the removal of physic-adsorbed water. (ii) The second weight loss stage, ranging 200 and about 548 °C, assigned to an initial dehydroxylation step. (iii) The last weight loss stage at a temperature higher than 650 °C resulting from sulfates decomposition, especially higher than 685 °C [25, 26].

DTA curves, reported in Fig. 3, yield complementary information. For DTA curves of Fig. 3a, the low exothermic peak at 341 °C should be assigned to the start of ZrO_2 crystallization while an dehydroxylation step went on; moreover, the exothermic peak at 451 °C demonstrated predominant crystallization of amorphous zirconium hydroxide resulting in crystalline ZrO_2 network. For DTA curves of Fig. 3b, the exothermic peak at 339 °C should be assigned to the beginning of ZrO_2 crystallization with contaminant dehydroxylation; meanwhile, other two exothermic peaks at 490 and 633 °C should also be assigned to ZrO_2 crystallization which was accomplished around 633 °C. So calcination at 650 °C will be necessary and helpful to complete the ZrO_2 crystallization process. It was reported that the crystallization of ZrO_2 was delayed by

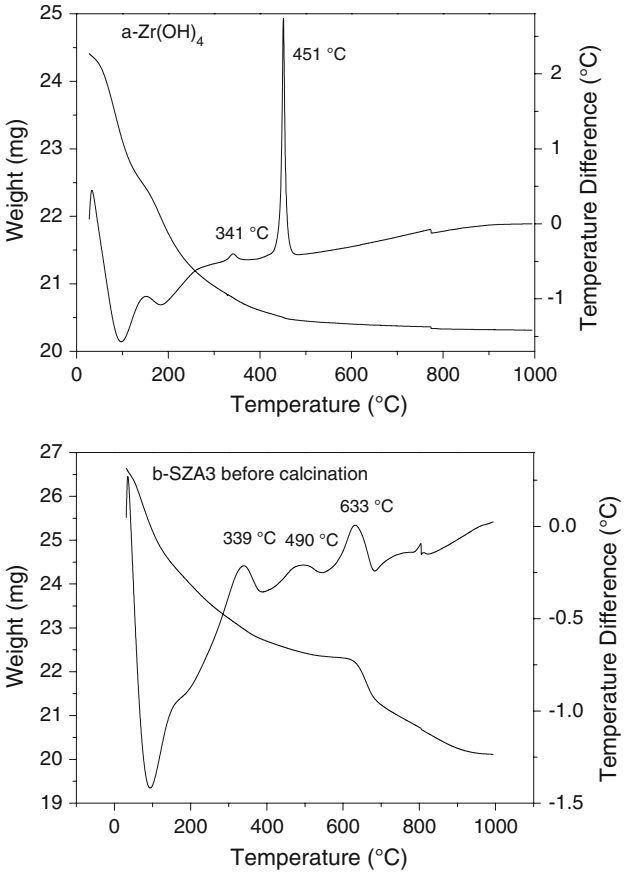

Fig. 3 TG-DTA profiles of $Zr(OH)_4$ and SZA before calcination

sulfated on amorphous Zr hydroxide [27]. The addition of alumina to zirconia can retard the transformation of metastable tetragonal zirconia phase into more stable monoclinic phase [28]. In addition, results in Fig. 3a and b revealed that alumina and sulfates in SZA3 samples must not only facilitate the start of ZrO_2 crystallization process but also extend the duration of this process.

3.4 Active Sites and Acidity

Sulfation of amorphous Zr hydroxide followed by calcination is necessary procedures to prepare an active SZ catalyst. In calcination step, structure rearrangement was performed to result in active sites containing sulfate groups that are attached to tetragonal zirconia. It was pointed out that only a small number of sulfate groups attached to ZrO_2 crystallites with high Miller-index would give rise to a few but very active sites [22]. Funamoto et al. [17] studied isomerization of *n*-butane over SZ catalyst. In their work, no hydrogen was used and no platinum loaded on SZ catalyst. Therefore, active sites resulting from acid properties on their catalysts were responsible for catalytic activity. A parallelism between its activity and the number of strong Lewis acid sites was observed.

Table 2 Acidity data of the catalysts from FTIR spectra of adsorbed pyridine

Desorption temperature (°C)	Acid amount (μmol g^{-1})	PSZA3-550	PSZA3-600	PSZA3-650	PSZA3-700
300	B-acid	27	26	23	14
	L-acid	84	117	158	113
	Tot-acid	111	143	181	127
400	B-acid	12	17	13	8
	L-acid	42	78	93	62
	Tot-acid	54	95	106	70
450	B-acid	12	12	9	6
	L-acid	41	62	70	44
	Tot-acid	53	74	79	50

FTIR characterization of pyridine adsorption was applied to determine the numbers of Lewis and Brønsted acid sites between 300 and 450 °C. Results were presented in Table 2. It showed that numbers of Lewis acid sites in the catalyst PSZA3-650 were 93 and 70 for pyridine relative amounts, desorbed at 400 and 450 °C, respectively. Corresponding numbers of them for PSZA3-600 were the second higher reaching 78 and 62. Comparing to that of the other two catalyst samples, these amounts were significantly higher. That was to say the number of strong Lewis acids for each of the four catalyst samples decreased in the order of: PSZA3-650 > PSZA3-600 > PSZA3-700 > PSZA3-550, which was in good agreement with changes in catalytic activities as shown in Sect. 3.1, indicating crucial role of strong Lewis acid sites and the optimum calcining temperature of 650 °C. Thermal analysis in Sect. 3.3 also shows that the calcining temperature of 650 °C is helpful to complete the crystallization process, and above 650 °C, the active sites would partly decompose resulting in sulfate removal as shown in Fig. 3 and activity loss. The activity decreased to a yield of 70% at calcination temperature of 700 °C as shown in Fig. 1.

Our results revealed that strong Lewis acid sites and tetragonal zirconia play the prevailing role for the activity of the PSZA3 catalysts prepared at varying SZA3 calcining temperatures, assuming that all other preparation parameters remained constant and a suitable calcination temperature will lead to form more active sites and tetragonal zirconia which are responsible for higher catalytic activity.

3.5 Surface Analysis by XPS Characterization

Zr 3d electron binding energy spectra for the four PSZA3 catalysts were presented in Fig. 4. It was seen that Zr 3d binding energy value of PSZA3-700 was the lowest, whilst that of PSZA3-550 was the highest with a decreasing order as: PSZA3-700 < PSZA3-650 < PSZA3-600 < PSZA3-550. Al 2p binding energy spectra of these four samples were shown in Fig. 5, which indicated that Al 2p electron binding energy is the highest for PSZA3-700, whilst the lowest for PSZA3-550 with an order of: PSZA3-700 > PSZA3-650 > PSZA3-600 > PSZA3-550. The binding energy of the Zr 3d5/2 in unpromoted ZrO_2 sample ranges between 182.2 and 182.5 eV [29, 30]. An obvious decrease in the binding energy of the Zr 3d in the case of PSZA3-700

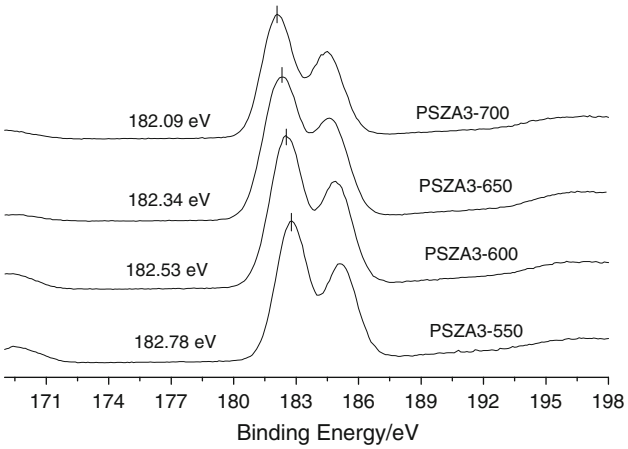

Fig. 4 Zr 3d binding energy of the PSZA catalysts

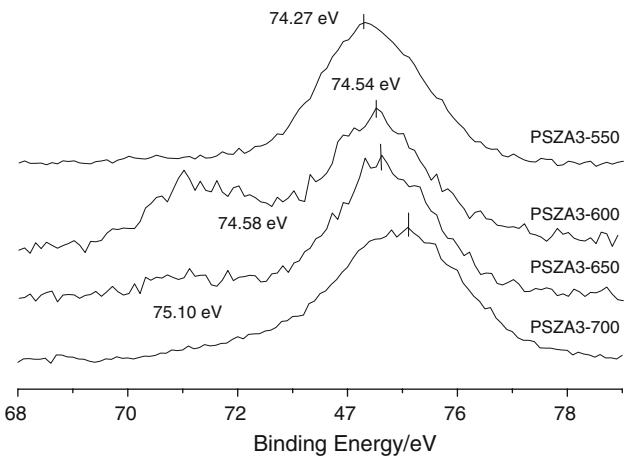

Fig. 5 Al 2p binding energy of the PSZA catalysts

(182.09 eV), in comparison to ZrO_2 alone. The binding energy of the Al 2p peak, in case of unpromoted Al_2O_3 samples, ranges between 74.2 and 74.7 eV [29, 30]. A obvious increase in the Al 2p binding energy can be noted for PSZA3-700 (75.10 eV) with respect to Al_2O_3. This indicates that alumina is strongly interacting with the zirconia at calcination temperature of 700 °C.

It was clear from Figs. 4 and 5 that Zr 3d binding energy decreased whilst that of Al 2p increased on increasing calcination temperatures, which shows that there is strong interaction between zirconia and alumina, and reveals that the electrons on Al^{3+} shifted to Zr^{4+}. Those resulted in better distribution of alumina into zirconia crystal that alleviated zirconia particle sintering and produced new acid centers after the calcination temperature increased from 550 to 650 °C as shown in Table 2. Meanwhile, sulfate decomposition and monoclinic crystal phase formation would be observed at exceeding calcining temperatures as shown in Fig. 2 and the thermal analysis results in Sect. 3.3.

3.6 TPR Analysis

TPR profiles of these four PSZA3 catalysts prepared at various SZA3 calcination temperatures are shown in Fig. 6. It is seen that only one peak with quite similar area appeared at each of these four traces. It was ascribed to the reduction of sulfate ions from the literatures [7, 31–33]. No peak was detected at temperature around 200 °C that resulted from Pt oxide reduction to metallic state [7]. Ebitani et al. [31, 32] suggested the absence of a distinct low-temperature reduction peak for platinum oxide can be because platinum is present as sulphide or sulphate that is harder to reduce. The Pt reduction is then delayed in the TPR, and is masked by the dominant sulphur reduction [33]. For the sample calcined at 550 °C (PSZA3-550), the peak minimum appeared at 494 °C, whilst that for the sample calcined at 600 and 650 °C they were at 468 and 451 °C, respectively. As for PSZA3-700, the peak appeared at 481 °C on the TPR pattern. The peaking temperature was increasing in the order as: PSZA3-650 < PSZA3-600 < PSZA3-700 < PSZA3-550, which was in correspondence to the catalytic activities.

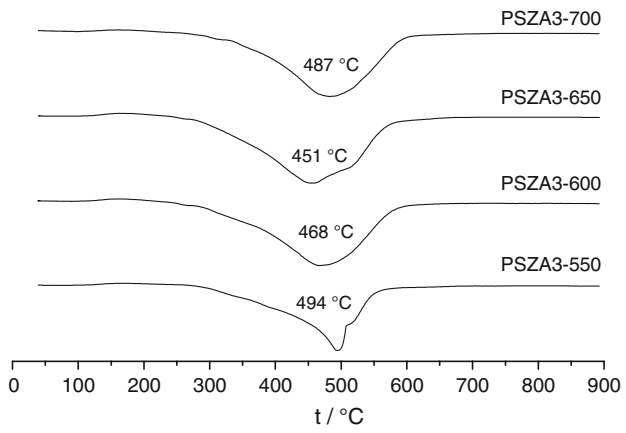

Fig. 6 H_2-TPR profiles of the samples

It was reported that transition metal, like Fe [34] and Ga [2] or Pt [33, 35] promoted SZ would possess higher sulphate reduction ability in H_2-TPR compared to SZ and the sulfate reduction ability was in line with catalytic activity. The differences in the sulfate reduction ability between various PSZA3 catalysts, however, might not result from platinum behaviours itself, because four SZA3 samples were calcined at varying temperatures, whereas the final calcination of all the four PSZA3 catalysts after Pt loading was performed at a fixed temperature viz. 525 °C in our PSZA3 catalyst preparation procedures. It is supposed that the lower the peak temperature of reduction of surface sulfates on the catalysts is, the more active the sulfates would be, and which would lead to more active sites as shown in Fig. 6 and Table 2. Therefore it was postulated that the differences would come from the surface property differences of the SZA3 catalysts after calcination, especially their surface acid properties. In H_2-TPR tests, there were possibilities that the stronger the SZA3 surface acid, the stronger its ability to obtain electron and thus the easier, its sulfate reduction by Pt action.

4 Conclusions

Calcination conditions show significant influences in the formation of the active sites of PSZA catalysts. Both the bonding of the sulfate anions to the surface of tetragonal zirconia and the interaction of alumina and zirconia contributed to the creation of active sites at suitable calcining temperature. XRD and TG-DTA analysis of the samples reveal that a suitable calcination temperature is helpful to complete the crystallization process of ZrO_2. An optimum calcination temperature also results in better distribution of alumina into zirconia crystal that alleviated zirconia particle sintering and produced new acid centers as shown in FTIR characterization of pyridine adsorption and XPS analysis and form more active sites which will have higher sulphate reduction ability as shown in H_2-TPR characterization. The catalytic activity varies with the calcination temperature in an order as PSZA3-650 > PSZA3-600 > PSZA3-700 > PSZA3-550, which is in line with the changes in strong Lewis acid sites. It was concluded from our work that changes in catalyst activity were in close agreement with that of the amounts of strong Lewis acid sites at varying calcination temperatures, assuming that all other preparation parameters remained constant.

Acknowledgements We would like to thank the financial supports from the key international cooperative research projects by National Ministry of Science and Technology, P.R. China (No. 2004CB720603).

References

1. Jatia A, Chang C, Macleod JD, Okubo T, Davis ME (1994) Catal Lett 25:21
2. Yori JC, Parera JM (1996) Appl Catal A 147:145
3. Cao CJ, Han S, Chen CL, Xu NP, Mou CY (2003) Catal Commun 4:511
4. Olindo R, Goeppert A, Habermacher D, Sommer J, Pinna F (2001) J Catal 197:344
5. Hua WM, Goeppert A, Sommer J (2001) J Catal 197:406
6. Haouas M, Walspurger S, Taulelle F, Sommer J (2004) J Am Chem Soc 126:599
7. Song XM, Sayari A (1996) Catal Rev Sci Eng 38:320
8. Kimura T (2003) Catal Today 81:59
9. Gao Z, Xia YD, Hua WM, Miao CX (1998) Top Catal 6:101
10. Watanabe K, Kawakamia T, Baba K, Oshioa N, Kimura T (2004) Appl Catal A 276:145
11. Paál Z, Wild U, Muhler M, Manoli J-M, Potvin C, Buchholz T, Sprenger S, Resofszki G (1999) Appl Catal A 188:257
12. Olindo R, Pinna F, Strukul G, Canton P, Riello P, Cerrato G, Meligrana G, Morterra C (2000) Stud Surf Sci Catal 130:2375
13. Hua W, Sommer J (2002) Appl Catal A 227:279
14. Sohn JR, Kim HW (1989) J Mol Catal 52:361
15. Comelli RA, Vera CR, Parera JM (1995) J Catal 151:96
16. Chuah GK, Jaenicke S, Cheong SA, Chan KS (1996) Appl Catal A 145:267
17. Funamoto T, Nakagawa T, Segawa K (2005) Appl Catal A 286:79
18. Hosoi T, Shimidzu T, Itoh S, baba S, Takaoka H, Kousaka T (1988) Am Chem Soc Div Petrol Chem Prep 33:562
19. Comelli RA, Canavese SA, Vaudagna SR, Figoli NS (1996) Appl Catal A 135:287
20. Lei T, Xu JS, Hua W, Tang Y, Gao Z (1999) Catal Lett 61:213
21. Sun Y, Walspurger S, Louis B, Sommer J (2005) Appl Catal A 292:200
22. Kim SY, Goodwin JG, Galloway D (2000) Catal Today 63:21
23. Vera CR, Pieck CL, Shimizu K, Parera JM (2002) Appl Catal A 230:137
24. Huang Y, Zhao B, Xie Y (1998) Appl Catal A 173:27
25. Moreno JA, Poncelet G (2001) Appl Catal A 210:151
26. Stichert W, Schüth F, Kuba S, Knözinger H (2001) J Catal 198:277
27. Comelli RA, Vera CR, Parera JM (1995) J Catal 151:96
28. Reddy BM, Sreekanth PM, Yamada Y, Kobayashi T (2005) J Mol Catal A: Chem 227:81
29. Wagner CD, Riggs WM, Davis LE, Moulder JF (1978) In: Muilenberg GE (ed) Handbook of X-ray photoelectron spectroscopy. Perkin-Elmer Corporation, Minnesota
30. Briggs D, Seah MP (eds) (1990) Practical surface analysis, auger and X-ray photoelectron spectroscopy, vol 1, 2nd edn. Wiley, New York
31. Ebitani K, Konishi J, Hattori H (1991) J Catal 130:257–267
32. Ebitani K, Konno H, Tanaka T, Hattori H (1993) J Catal 143:322–323
33. Løften T, Blekkan EA (2006) Appl Catal A 299:250
34. Henao JD, Wen B, Sachtler WMH (2005) J Phys Chem B 109:2055
35. Xu BQ, Sachtler WH (1997) J Catal 167:224